J Mater Sci
DOI 10.1007/s10853-013-7450-2

The migration and formation energies of N-interstitials near [001] Fe surfaces: an ab initio study

L. Autry · R. Ramprasad

Received: 5 February 2013 / Accepted: 16 May 2013

Abstract Using density functional theory, the mechanism of surface segregation of N to the [001] Fe surface was studied. The formation and migration energies were decomposed into chemical bonding and strain energy components. While the segregation energy was determined to be −1.1 eV, the bonding and strain energy components for segregation were −0.5 and −0.6 eV, respectively. The results indicate that strain energy relaxation plays a major role in surface segregation, and that there is approximately a 7-layer transient region, which separates bulk and surface environments. The role of the strain energy on interstitial migration barriers was also critically evaluated.

Introduction

The interactions of adsorbed atoms with free surface defects affect the chemical affinity of the surface, influencing surface phenomena such as adhesion [1], catalysis [2], and tribology [3]. Typically, surfaces have a different concentration of substitutional or interstitials alloying elements compared to the bulk. When the concentration at the surface is higher than in the bulk, the alloying element is said to have segregated to the surface. Experimentally, it has been demonstrated that non-metal interstitial defects [4] and metallic substitutional elements [5] will migrate toward clean surfaces in high-vacuum environments. In order to control surface properties better, the mechanisms of surface segregation need to be better understood. It has been proposed that the enthalpy of segregation for an alloying element is a combination of strain energy relief and chemical passivation of the dangling surface bonds [6].

In order to understand the theoretical underpinnings of surface segregation, researchers have used empirical approaches such as fitting thermodynamic models to segregation measurements [7]. The first atomic modeling attempts (pre-1990) to predict segregation used tight binding methods [8, 9], muffin-tin methods [10], and density functional theory (DFT) approaches [11]. Using tight binding predictions and preexisting experimental data, Abraham [12, 13] developed a method based on the specific surface energy ratio and the atomic size ratio to predict the segregating element of a binary substitutional alloy. This was the first study in which the segregation phenomenon was related to the strain energy created by an alloying element in the bulk. Jellium approaches [14] later confirmed that in a binary, substitutional, solid solution the atom with the larger atomic radius segregates to the surface. Modern pseudopotential [15–17] calculations can routinely estimate the 0 °K segregation enthalpy for various substitutional and interstitial alloy systems. To date, however, there has not been a first-principles evaluation of the strain energy contribution to segregation.

In this paper, DFT is used to map out the energies of an interstitial N atom near the {100} surface of BCC Fe. Site energies are determined, along with activation energies for site-to-site migration. The formation and migration energies are separated into their bonding and strain energy components. The results illustrate that strain energy plays a large role in the segregation and migration barrier energies. It was also revealed that there is a ∼7-layer transient region between the surface and bulk environments.

L. Autry (✉) · R. Ramprasad
Department of Chemical, Materials and Biomolecular Engineering, Institute of Materials Science, University of Connecticut, 97 North Eagleville Road, Storrs, CT 06269, USA
e-mail: Autch97@gmail.com

Published online: 25 June 2013

Methodology

DFT calculations were carried out using the Vienna ab initio simulation package [18]. The ion–electron interaction was handled using Vanderbilt ultrasoft pseudopotentials [19]. The Perdew–Burke–Ernzerhof generalized gradient approximation was used to handle the quantum mechanical part of the electron–electron interactions (namely, the exchange–correlation interaction). All calculations involved explicit treatment of electron spin. Brillouin zone integrations were carried out using the tetrahedron method [20]. To improve convergence, Fermi-level smearing via Methfessel–Paxton [21] was carried out. A 0.05 eV/Å force cut-off was used during ionic relaxation, and a 0.001 eV convergence criterion was used for the electronic minimization steps. Bulk calculations (involving the primitive cell) required a Monkhorst–Pack k-point mesh of 12 × 12 × 12, which was proportionately decreased for the larger supercell and slab calculations.

Table 1 summarizes the results of calculations performed to validate our adopted procedure, and lists the computed lattice parameter of Fe, its surface energy, magnetic moment, and the N-interstitial formation energies at two possible sites. As can be seen, the calculated bulk quantities agree with previously determined values.

The {001} surface energy versus number of layers in the slab was determined in order to ascertain how many layers were needed to accurately model the [001] BCC Fe surface. The convergence of the surface energy was achieved after 4-layers, and was determined to be 2.32 J/m^2 with an oscillation of 0.050 J/m^2.

In order to study the N-interstitial formation energies in the near-surface region a 10-layer {001} BCC iron slab was used. The number of atoms per layer required in the slab model was determined by calculating the bulk N-interstitial formation energy versus cell size. It was determined that the N-interstitial formation energy decreased by less than 8 % going from a 2 × 2 × 2 supercell to a 4 × 4 × 4 supercell. In order to save on computation time, the size of each layer in the x and y directions was set to 2 × 2. For the migration and interstitial formation energy calculations, this is a reasonable approach because the slab calculations were compared directly. The size of the slab used in these migration calculations was 2 × 2 × 5 with a vacuum gap of 10 Å. The segregation energy for incorporating N on the surface or in the near-surface regions was referenced to the octahedral formation energy using the 3 × 3 × 3 bulk supercell. To directly evaluate the effect of a free surface on the interstitial formation energy of an N atom on the octahedral site in a 2 × 2 × 5 supercell with a 10 Å vacuum gap, a 2 × 2 × 5 supercell without a vacuum gap was used to calculate the bulk octahedral site formation energy.

The N migration activation barriers in the bulk and near the {100} surface were studied using the nudged elastic band (NEB) method [26]. Three images were used on all NEB calculations except for the 1st–2nd layer in which five images were used.

Table 1 Preliminary BCC Fe and BCC Fe + N interstitial calculations

Quantity	This work	Past work
Lattice parameter (Å)	2.85	2.834
		2.87 [22]
{100} Surface energy (J/m^2)	2.32	2.47 [23]
Bulk magnetic moment (μ_B/atom)	2.26	2.22 [24]
N-interstitial formation energy (eV/atom)		
Octahedral	−5.27	−5.196 [25]
Tetrahedral	−4.51	−4.407 [25]

Results and Discussion

The interstitial formation energy and its dependence on strain energy

The interstitial formation energy is given by:

$$E_{\text{form}} = E_{\text{cell+N}} - \left\{E_{\text{cell}} + E_{\text{N}}^{\text{iso}}\right\} \quad (1)$$

E_{cell} is the energy of a relaxed Fe supercell. $E_{\text{N}}^{\text{iso}}$ is the energy of the isolated N atom, and $E_{\text{cell+N}}$ is the relaxed energy of the Fe supercell with an N atom inserted.

Strain energy plays a major role in the interstitial formation energy whether one is doing calculations on bulk or on surface systems. When an N atom is inserted into the octahedral site, it produces a tetragonal distortion in the surrounding lattice.

The associated strain energy can be determined by performing a self-consistent calculation on the distorted lattice with the N atom removed. It is important to emphasize that the interstitials distort the supercell lattice parameters as well as the atoms within the supercell. In the calculations herein only the atomic distortion is considered; thus the strain energy calculated in this study cannot be considered as the actual strain energy caused by an interstitial. The energy of a distorted cell is given by $E_{\text{cell}}^{\text{dist}}$. The strain energy is then given by:

$$E_{\text{strain}} = E_{\text{cell}}^{\text{dist}} - E_{\text{cell}} \quad (2)$$

Thus, the interstitial formation energy has two components: a strain component related to the distorted Fe–Fe bonding (E_{strain}) and a chemical bonding component related to formation of Fe–N bonds (E_{Bond}). Therefore, in the relaxed configuration, the interstitial formation energy is given by:

$$E_{\text{form}} = E_{\text{bond}} + E_{\text{strain}} \quad (3)$$

Note that E_{bond} and E_{strain} will have opposite signs unless the interatomic distance is small, in which case E_{bond} will be positive. The bonding energy, E_{bond}, is the energy required to remove the N atom from the relaxed configuration. This is given by:

$$E_{\text{bond}} = E_{\text{cell+N}} - \left\{E_{\text{cell}}^{\text{dist}} + E_{\text{N}}^{\text{iso}}\right\} \quad (4)$$

The strain energy is a positive quantity, which raises the energy of the system due to the work being done. Equation (1) for the relaxed state is recovered if (2) and (4) are substituted into (3).

Applying the above equations to bulk interstitials using $2 \times 2 \times 2$ Fe + N(oct.) and $3 \times 3 \times 3$ Fe + N(oct) supercells give the results shown in Table 2. Note that $A \times B \times C$ Fe + N(oct) means an $A \times B \times C$ Fe cell with N added to the octahedral site. A surprising result is that the strain energy associated with the interstitial distortion in the tetrahedral location is lower than that in the octahedral location. The higher strain energy associated with the octahedral position is compensated for by forming stronger Fe–N bonds during the relaxation process, which results in a more favorable E_{bond} value for the octahedral position. In the octahedral and tetrahedral $2 \times 2 \times 2$ Fe + N(oct or tet) cells, the strain energy is about 16 % of the formation energy; thus the role of strain energy in the energetics of interstitials is important. In regards to cell size, the amount of strain energy decreases in both octahedral and tetrahedral interstitial symmetries as the supercell size increases going from a $2 \times 2 \times 2 \rightarrow 3 \times 3 \times 3$ cell. This is because the Fe atoms are able to relax more completely with a larger cell and results in a lower cell pressure. Thus, the E_{bond} in the $3 \times 3 \times 3$ cells is larger due to the ability of the Fe atoms to relax more. However, a very important point is that no matter how large the supercell is, the strain never disappears since the strain energy is based on the displacements of the iron atoms from their lattice sites.

Bulk diffusion studies

For a BCC lattice, there are three symmetrically inequivalent jump paths for octahedral-site-to-octahedral-site migration. The crystallographic plane and direction for these jumps are: Path 1 {100}| [100], Path 2 {100}| [110], and Path 3 {110}| [111]. Figure 1a shows these paths. Figure 1b shows the results of the NEB calculations using these paths as initial guesses. After relaxation, Path 1 stays on [100] plane and in the [100] direction. Path 2 relaxes into a path that can be made up of two Path 1 jumps: the 4th image relaxes into an octahedral site, while the 2nd and 6th images relax into tetrahedral sites. Path 3 stays on the {110} plane and in the [111] direction. Path 1 and Path 3 give two possible saddle points, but since Path 1 has a lower activation barrier by a factor of almost two (0.767 eV for Path 1 and 1.414 eV for Path 3) the likely diffusion pathway will be along {100}| [100]. The activation barrier for Path 1 is close to the 0.77 eV value determined by Domain et al. [27]. Since Path 1 is the likely diffusion pathway in this system it is the only path considered in the migration studies close to the (001) surface.

The components of the migration energy are plotted in Fig. 1c according to Eqs. (2) and (4). As expected, the saddle point had lower strain energy, but higher bonding energy. This is because the saddle point is the tetrahedral site. The strain energy was highest in the image adjacent to the saddle point; however, the bonding energy compensated for this giving lower formation energy. Thus in the case of bulk diffusion the activation barrier is controlled by the increase in the bonding energy at the tetrahedral site. Reproducing Fig. 1c with the larger $3 \times 3 \times 3$ cell revealed that the strain energy peak at the tetrahedral site was lower by 0.11 eV, the binding energy was lower by 0.04 eV, and the formation energy was lower by 0.07 eV. This indicates that the cell size did not affect the profiles of the energy components so one can still garner useful information while using a smaller cell size at the expense of some accuracy.

In order to directly compare a bulk environment to a near-surface environment, a $2 \times 2 \times 5$ Fe + N(oct) bulk supercell as described in the "Methodology" section was used to calculate the migration energies along Path 1 in the [001] direction. The N formation energies were also determined for the two symmetrically inequivalent octahedral sites (see Fig. 2a) that are labeled as the A-sites and B-sites. An N atom in the A-site induced a tetragonal distortion along the [100], [010] directions, and a B-site N atom induces a distortion along the [001] direction. Since the supercell is elongated in the [001] direction, A-sites and B-sites are symmetrically inequivalent. The interstitial formation energies for A-sites and B-sites are −5.17 and −5.55 eV, respectively; the corresponding formation energy in the bulk for the $3 \times 3 \times 3$ cell was −5.31 eV (see Table 2). The activation barrier along Path 1 for the $2 \times 2 \times 5$ Fe + N(oct) cell is 0.59 eV, and for the bulk $3 \times 3 \times 3$ cell it was 0.63 eV.

Table 2 Bulk N-interstitial formation energies separated into bonding and strain components

Cell	E_{Form} (eV)	E_{strain} (eV)	E_{Bond} (eV)
$2 \times 2 \times 2$ Fe + N(oct)	−4.89	0.91	−5.80
$2 \times 2 \times 2$ Fe + N(tet)	−4.16	0.37	−4.52
$3 \times 3 \times 3$ Fe + N(oct)	−5.31	0.73	−6.05
$3 \times 3 \times 3$ Fe + N(tet)	−4.68	0.31	−4.99

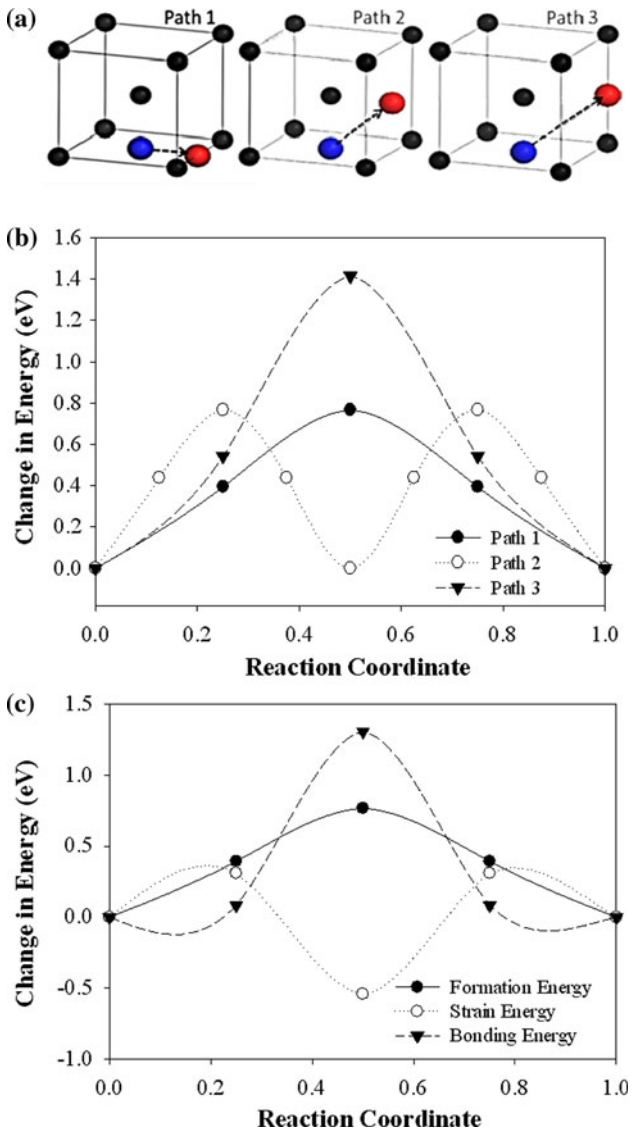

Fig. 1 The bulk diffusion paths and activation energies for N-diffusion. **a** The three symmetrically inequivalent jump paths for the N octahedral interstitial. **b** NEB results for each jump path. Energies are taken relative to the 2 × 2 × 2 Fe, octahedral N cell energy. **c** The energy change along Path-1 broken down into bonding and strain components

Fe slab formation energy studies

The relaxed N-interstitial formation energies versus position in the 10-layer slab are shown in Fig. 2b. The formation energy is given by (1). These values are compared to the values calculated for the bulk 2 × 2 × 5 40Fe + N(oct) supercell in the previous section. As before, due to the asymmetry of the supercell, there are two unique octahedral sites, which are labeled as the A-sites and B-sites. As with the bulk supercell, the B-site is more stable than A-site. Clearly, the N atom prefers to be on the surface in the B-site (hollow site); the A-site (bridge site) on the surface was found to be an unstable position with respect to displacements in the [001] direction and hence never converged. Jiang et al. [28] performed calculations which involved the adsorption of C on Fe surfaces; they too determined that the hollow site was stable. The interstitial formation energy on the surface was ∼−6.5 eV. The interstitial formation energies approached the corresponding bulk values for the 2 × 2 × 5 Fe + N(oct) bulk supercell (see "Bulk diffusion studies" section) as the atom went deeper into the slab. At the 5th monolayer, the interstitial formation energies for the A-site and the B-site are −5.059 and −5.450 eV, respectively. These values are close to their bulk value counterparts in the 2 × 2 × 5 bulk supercell: −5.178 and −5.553 eV. Both values are close to 2 % of their bulk values. To determine how many layers deep an interstitial atom needs to go in order to be in a bulk-like environment a larger supercell was needed. Interstitial formation energy calculations were done on a 2 × 2 × 7 Fe + N(oct) slab with a 10 Å vacuum gap and a 2 × 2 × 7 Fe + N(oct) bulk supercell. The interstitial N formation energies on the 7th layer were −5.142 and −5.515 eV for the A-site and B-site, respectively. These values are very close (less than 1 %) to their 2 × 2 × 7 Fe + N(oct) bulk counterparts: −5.182 and −5.563 eV. It appears that the formation energies may approach their bulk values asymptotically as the N atom moves away from the surface. The 0 °K heat of segregation was −1.1 eV where the bulk reference was a 3 × 3 × 3 supercell.

The E_{bond} (relaxed) and E_{strain} components are both plotted against the layer position in Fig. 2b. Importantly, the bonding energy is not a strong function of interstitial position; as the migration driving force (the formation energy) changes only the strain energy changes. An interesting observation is that the interstitial formation energies for layers 2–5 are higher than the bulk values. This is due to the extra strain energy associated with the interstitial in those locations. As can be seen in Fig. 2b, the strain energy rises as the N atom moves closer to the surface. When the N atom is at the surface there is zero strain energy since the interstitial is not causing a distortion. The strain energies also indicate why the B-site is more stable than the A-site. For interstitial positions between layers 2–5, the strain energy for the B-site is on average 0.310 eV lower than that of the A-site. The interaction of the neighboring supercell images when the interstitial is in the A-site prevents some relaxation of the distorted iron atoms, which artificially raises the interstitial formation energy due to the increased cell pressure. For that reason, to determine the segregation energy the N-interstitial formation energies of a 3 × 3 × 5 Fe + N(A-site) slab (with 10 Å vacuum gap) and a 3 × 3 × 3 Fe + N(oct-site) were compared. For the segregation energy components, there was a −0.6 eV change in strain energy and a −0.5 eV change in bonding

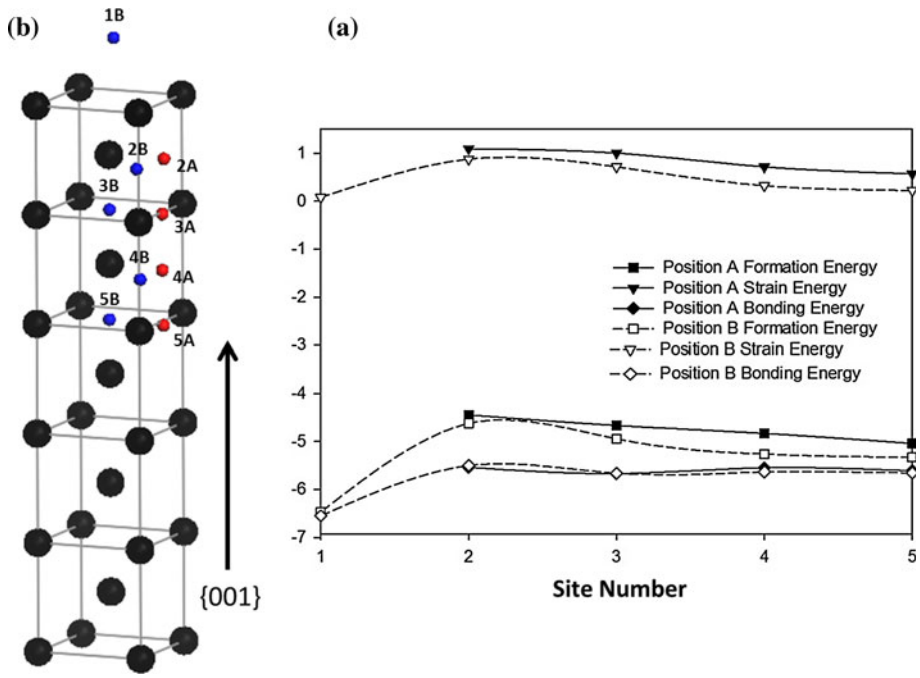

Fig. 2 The site formation energies for A-site and B-site positions along the [001]-direction from the surface. **a**, **right** Interstitial formation energy and it's components as a function of distance from the surface of the {001} BCC Fe slab. **b**, **left** Illustration of the bulk 2 × 2 × 5 slab used in these calculations. The different interstitial locations are indicated on this figure

energy going from the bulk 3 × 3 × 3 Fe + N(oct) supercell octahedral site to the 3 × 3 × 5 Fe + N slab surface hollow site.

Layers 2–5 are a transient region, which separates the surface environment from the bulk environment. The reason for this transient region is that the N-interstitial interferes with the surface relaxation associated with free surfaces. Therefore, in addition to strain energy component caused by the tetragonal distortion, there is a strain energy component because the surface/subsurface layers cannot fully relax. Table 3 illustrates the interlayer distances with and without the N-interstitial inserted into the slab. Note that the interlayer distances for the 2 × 2 × 5 Fe + N(oct) supercell are calculated by averaging the (001) coordinate for each atom in each layer. The differences of the averaged coordinates are then determined between each layer. It is evident that the N atom causes almost no strain in the [001] direction when it is at the 1B-site. However, when the N atom is in the 2A-site, most of the strain is caused along the [001] direction—specifically between layers 1 and 2. This is because the layer spacing between layers 1 and 2 contracts the most in the N-free supercell. Hence, it is to be expected that an N atom placed in between these layers will cause the most distortion.

The fact that the bonding energy is not a strong function of position in the slab is an important point to bring up. Throughout the migration of the interstitial to the surface the coordination number (twofold) of the N atom does not change until it reaches the surface (fourfold). The slight variations between sites 2–5 are due to the different amounts of relaxations in the Fe atoms. At the 1B-site, the bonding energy is ~0.8 eV lower than the bonding energy in the bulk. This is due to two effects: the increased coordination number at the surface and the near-zero strain energy.

N migration activation energies in near-surface region

For the 2 × 2 × 5 bulk Fe–N supercell the transition energy for the A-site-to-A-site jump is 0.591 eV. Figure 3 shows the activation barriers for N migration in the near-surface region. Except for the 1st–2nd layer jump (B-site to A-site), the inward migration involves A-site-to-A-site jumps. The activation energy barrier profile for the jump between the 1st and 2nd layer displayed a plateau and a subsequent sharp peak. This profile was observed by Jiang et al. for carbon migration from the {001} BCC Fe surface to the next layer down. The activation energy barriers approach the bulk value of 0.591 eV as the N atom goes deeper into the slab. The activation barriers going from the surface (in eV) are: 2.706 for 1st–2nd layer jumps, 0.715 for 2nd–3rd layer jumps, 0.667 for 3rd–4th layer jumps, and 0.616 for 4th–5th layer jumps. Obviously, adding more layers will allow the bulk activation energy barrier to be more closely approached. According to Fig. 3, the rate-limiting jump is controlled by the strain energy the N atom injects into the surface during the transition process. The bonding energy increase does not play a role until the atom starts to move beyond the 2nd layer.

The rather high activation energy barrier for 1st–2nd layer jump indicates that the initial penetration of N into the iron crystal is the rate-limiting step for surface to bulk

Table 3 Interlayer distances without N added (ref.) and with N added to the sites along the diffusion path

	Interlayer spacing			
	Layers 1–2	Layers 2–3	Layers 3–4	Layers 4–5
Ref	1.390	1.464	1.437	1.406
1B	1.397 (0.005)	1.458 (0.004)	1.435 (0.002)	1.403 (0.002)
2A	1.528 (0.099)	1.456 (0.006)	1.420 (0.012)	1.439 (0.023)
3A	1.400 (0.007)	1.569 (0.072)	1.453 (0.011)	1.417 (0.008)
4A	1.404 (0.005)	1.468 (0.007)	1.523 (0.061)	1.424 (0.015)
5A	1.395 (0.004)	1.476 (0.008)	1.446 (0.006)	1.479 (0.052)

The interlayer strains are provided in the parentheses. Note that the interlayer spacing values are based on layer-averaged atomic positions

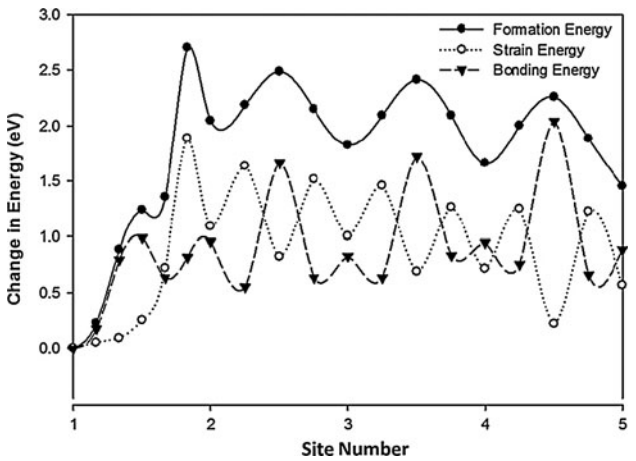

Fig. 3 Activation energy barriers for migration into the {001} BCC Fe slab. Five images were used for the 1st–2nd layer transition and three images were used for the rest

diffusion. For diffusion going to the surface from the bulk the activation energy barriers are: 0.712 for 5th–4th layer jumps, 0.772 for 4th–3rd layer jumps, 0.742 for 3rd–2nd layer jumps, and 0.941 for 2nd–1st layer jumps. These results indicate that the 1st–2nd layer jump is the rate-limiting step for diffusion in either direction. It is interesting to note that B-site is the more stable position for an N atom, but N-diffusion along the [001] occurs by jumps between A-sites. A near-surface lattice model modeling diffusion would have to consider the A-site to B-site jumps at each layer until the atom is sufficiently far from the surface.

Surface segregation is equally appropriately viewed as a kinetic phenomenon as it is an equilibrium phenomenon. The large activation barrier between sites 1 and 2 caused by the strain energy increase "trap" the N atoms on the surface leading to a net accumulation of N atoms relative to the bulk. Models used to predict surface segregation, such as the Langmuir–McLean relationship rely on solely determining the heat of segregation, which is appropriate for equilibrium calculations. However, the physical phenomenon of surface segregation is best described through a kinetic viewpoint. Briefly consider a three-state system where the law of mass action describes the kinetic processes:

$$r_{AB} = \alpha_{AB} \exp(Q_{AB}/RT)\, C_A \tag{5}$$

where r_{ab} is the jump rate between states A and B, Q_{AB} is the activation barrier between states A and B, and C_A is the concentration in state A. At equilibrium $r_{AB} = r_{BC}$ and $r_{CB} = r_{BA}$. In addition, using the extreme condition that the enthalpies of states A and C are equal gives an expression for the relative concentrations between those states:

$$\frac{C_C}{C_A} = \frac{\alpha_{BA}\alpha_{BC}}{\alpha_{CB}\alpha_{AB}} \exp\left[\frac{2}{RT}(Q_{CB} - Q_{AB})\right] \tag{6}$$

What this is implying is that even when there is no segregation energy a concentration difference between states A and C can exist. In this situation, surface segregation is a consequence of the entropy increase related to diffusion rather than an enthalpy change. Segregation models based on surface to near-surface activation barriers are rare, but kinetic modeling of this type can give information on how the system evolves, and the final state of the system.

Conclusions

A comprehensive study of the mechanisms underlying the segregation of N-interstitials to the [001] surface of Fe has been performed using first principles computations. Our conclusions may be summarized as follows:

1. The N-interstitial formation energy was separated into strain and bonding energy components. The strain energy component was based on how much the interstitial distorted the supercell during ionic relaxation. It was concluded that the octahedral interstitial site was more stable than the tetrahedral site because of the higher bonding energy contribution. The tetrahedral site created less strain energy than the octahedral site. The tetrahedral site's bonding energy, however, was higher.
2. The driving force for surface segregation is a combination of bonding energy and strain energy. At the surface, it was determined that the strain energy was the smallest and the bonding energy contribution was the most negative. This indicates that strain relief contributes largely to surface segregation.
3. Between the surface environment and the bulk environment there is a transient region where the migrating

interstitial interferes with surface relaxation thus causing additional strain to the system. In this region, the interstitial formation energy is higher than in the bulk. Within 7 layers from the surface, the interstitial formation energy is less than 1 % of the bulk value.

4. At the saddle point in bulk interstitial diffusion, the strain energy is at a minimum while the bonding energy is at a maximum. The same trend follows during the migration from the [001] surface to the bulk; however, the strain energy profile is shifted to a higher value than it is in the bulk while the bonding energy remains approximately unchanged.
5. The surface to 2nd layer activation barrier, which is dominated by an increase in strain energy, limits the diffusion rate to the surface. As the N atom moved deeper into the slab, the activation barrier approached its bulk counterpart.

Acknowledgements I would like to thank Dr. Harris Marcus for providing me the funding to do this study through the Institute of Materials Science of the University of Connecticut.

References

1. Wachowicz E, Kiejna A (2008) Comput Mater Sci 43:736
2. Calvin H (2001) Appl Catal A Gen 212:17
3. Tarkowski P, Budzynski P, Kasietczuk W (2005) Vacuum 78:679
4. Grabke HJ, Paulitschke W, Tauber G, Viefhaus H (1977) Surf Sci 63:377
5. Van Langeveld AD, Ponec V (1983) Appl Surf Sci 16:405
6. Dowben P (1990) Allen Miller surface segregation phenomena. CRC Press, Boca Raton
7. Seah MP (1979) J Catal 57:450
8. Foiles SM (1985) Phys Rev B 32:7685
9. Tomanek D, Aligia AA, Balseiro CA (1985) Phys Rev B 32:5051
10. Balseiro CA, Morán-López JL (1980) Phys Rev B 21:349
11. Muscatt JP (1982) J Phys C Solid State Phys 867:867
12. Barnett RN, Uzi Landman CL (1983) Phys Rev B 28:6647
13. Abraham FF (1981) Phys Rev Lett 46:546
14. Abraham FF, Nan-Hsiung T, Pound GM (1979) Surf Sci 83:406
15. Yamauchi H (1985) Phys Rev B 31:7688
16. Yamaguchi M, Nishiyama Y, Kaburaki H (2007) Phys Rev B 76:035418
17. Ponomareva AV, Isaev EI, Skorodumova NV, Vekilov YK, Abrikosov IA (2007) Phys Rev B 75:245406
18. Kresse G, Furthmüller J (1996) Comput Mater Sci 6:15
19. Vanderbilt D (1990) Phys Rev B 41:7892
20. Blöchl P, Jepsen O, Andersen OK (1994) Phys Rev B 49:16223
21. Methfessel M, Paxton AT (1989) Phys Rev B 40:3616
22. Jiang DE, Carter EA (2003) Surf Sci 547:85
23. Cullity BD (2001) Elements of X-ray diffraction, 3rd edn. Prentice Hall, Upper Saddle River
24. Błoński P, Kiejna A (2007) Surf Sci 601:123
25. Kittel C (1996) Introduction to solid state physics, 7th edn. Wiley, New York
26. Henkelman G, Jóhannesson G, Jónsson H (2002) Prog Theor Chem Phys 5:269
27. Domain C, Becquart CS, Foct J (2004) Phys Rev B 69:144112
28. Jiang DE, Carter EA (2005) Phys Rev B 71:045402